Two-Nucleon Phase-Shift-Set Discrimination by Means of the Binary Optical Potential*†

JOSEPH S. CHALMERS‡ AND ALVIN M. SAPERSTEIN
Department of Physics, Wayne State University, Detroit, Michigan
(Received 4 December 1967)

The scattering of nucleons from light nuclei at energies of 142, 210, and 310 MeV is calculated using the multiple-scattering optical potential obtained by retaining all terms which are binary or less in the two-nucleon amplitudes. The binary potential includes the impulse-approximation correction as well as the double-scattering correction. Nucleon-nucleus scattering observables are computed, using optical potentials calculated with some of the Yale and Livermore phase-parameter sets and the Fermi and Brueckner-Gammel nuclear-correlation functions. The observables are compared with data in an effort to ascertain the differences caused by changing N-N scattering phase parameters and/or nuclear-correlation functions and to see whether it is feasible to use such changes in attempts to pin down N-N and nuclear parameters.

I. INTRODUCTION

THERE have been many attempts[1–3] to make a selection among proposed models of the two-nucleon force by means of nucleon-nuclear data. Using the very small-angle scattering data at 300 MeV, Bethe[1] showed that the nucleon-nucleus differential cross section and polarization could not distinguish between the different sets of N-N scattering phase parameters then current. This result was to be expected since the forward N-N amplitude is mostly imaginary and hence determined by the total cross section, a quantity which is presumably well fit by all acceptable phase-shift sets. With the failure of the forward-scattering data to discriminate between phase-shift sets, interest arose[3] in the possibility that finite-scattering angle data would allow such a differentiation. We[4] have recently made such a comparison, computing an optical potential from single scattering of the incident nucleon with nucleons in the nucleus. Using the Yale[5] and Livermore[6] two-nucleon phase-shift sets, we found significant differences between the nucleon-nucleus scattering observables at finite angles as computed with different phase-shift sets. In fact, we found the Yale set to give a superior fit to the data at incident lab energies of 142, 210, and 310 MeV. However, when computing large-angle nucleon-nucleus scattering, we expect that multiple scattering should add important terms to the optical potential, especially at the lower energies. It thus becomes important to see what the multiple-scattering effects are, and whether or not they will obscure the differences previously found between different sets of phase shifts. Specifically, in order to compute the double-scattering contribution to the optical potential, we must know the N-N correlation function within the nucleus. Does the lack of knowledge of this nuclear-structure function hinder the attempt to use elastic nucleon-nucleus scattering experiments to differentiate between different N-N parameters or can such experiments contribute both to the desired parameter discrimination *and* some knowledge of nuclear correlations? We explore this question in this paper.

Watson[7] has given a formalism in which the optical potential is expressed in terms of two-nucleon scattering amplitudes as an expansion representing contributions from single, double, and higher-order scatterings of the incident nucleon by the nuclear nucleons. The double-scattering term of this expansion was evaluated in an approximate form by Johnston and Watson,[8] and used by McDonald and Hull[9] to calculate the double-scattering correction to the optical potential in terms of the Yale phase-shift set. McDonald and Hull found that the addition of the double-scattering term to the single-scattering potential significantly affected the nucleon-nuclear observables at 142 MeV, and decreasingly so at higher energies.

In the present work, we evaluate all terms in the optical potential which are binary or less in the two-nucleon scattering amplitudes. This will require the evaluation of both the double-scattering correction, previously used in an approximate form by McDonald and Hull,[9] and the impulse-approximation correction. The binary-optical potential will be evaluated in terms of the Yale and Livermore phase-parameter sets and

* Work partly supported by the National Science Foundation under Contract Nos. GP-5077 and GP-7853.

† Submitted to the Office for Graduate Studies, Graduate Division of Wayne State University, Detroit, Mich. in partial fulfillment of the requirements for the Ph.D. degree by J. S. Chalmers.

‡ Present address: Department of Physics, University of Louisville, Louisville, Ky.

[1] H. A. Bethe, Ann. Phys. (N. Y.) 3, 190 (1958).

[2] A. H. Cromer, Phys. Rev. 113, 1607 (1959).

[3] A. M. Saperstein and D. Feldman, Nuovo Cimento 14, 457 (1959).

[4] J. S. Chalmers and A. M. Saperstein, Phys. Rev. 156, 1099 (1967).

[5] G. Breit, M. H. Hull, Jr., K. E. Lassila, K. D. Pyatt, Jr., and H. M. Ruppell, Phys. Rev. 128, 826 (1962); M. H. Hull, Jr., K. E. Lassila, M. H. Ruppell, F. A. McDonald, and O. Breit, *ibid.* 128, 830 (1962). Sets YLAM and YLAN3M were used, and are henceforth referred to as the "Yale set." The most recent Yale phase-shift sets [G. Breit, Rev. Mod. Phys. 39, 560 (1967)] were not made available to us at the time this work was being done.

[6] R. A. Arndt and M. A. MacGregor, Phys. Rev. 141, 873 (1966). The energy-independent phases were used.

[7] K. M. Watson, Phys. Rev. 105, 1388 (1957).

[8] R. R. Johnston and K. M. Watson, Nucl. Phys. 28, 583 (1961).

[9] F. A. McDonald and M. H. Hull, Jr., Phys. Rev. 143, 838 (1966).

used to calculate the nucleon-nuclear observables. An attempt will then be made to choose between these sets on the basis of the nucleon-nuclear data.

Since the evaluation of the binary-optical potential requires knowledge of the nuclear-correlation function, knowledge which is not readily available, we must also investigate the effect of using different forms for this function. The integral over the correlation function, which arises in the evaluation of the binary potential, will be evaluated directly rather than being approximated by correlation lengths as was done in Refs. 8 and 9. In evaluating the binary potential, we will relax the forward-scattering approximation which was made in Refs. 8 and 9. As a further correction, we improve the very-small-angle part of the nucleon-nuclear amplitudes used in the single-scattering part of the optical potential by including contributions of the one-pion exchange tail. The optical potential thus found will be used in its momentum-space representation to solve the partial-wave integral scattering equation for the scattering of nucleons by He^4, C^{12}, O^{16} at energies of 142, 210, and 310 MeV. The method of solution and the manner in which Coulomb effects are included are given in some detail in Ref. 4.

In Sec. II, we discuss the evaluation of the optical potential. Section III describes the quantitative effects of the various parts of the potential on the observables, elastic nucleon-nucleus differential cross section and polarization. In Sec. IV, the calculations are compared with data, and the Yale and Livermore sets compared on this basis. This section also includes an empirical choice between two models of the nuclear-correlation function. Section V considers the various factors in the calculation which affect agreement with experiment, and in Sec. VI our conclusions are drawn.

II. OPTICAL POTENTIAL

The Watson[7] expansion for the optical potential is given as an expectation value over the nuclear ground state $|0\rangle$ by

$$V=\langle 0|\sum_{i=1}\tau_i+\sum_{\substack{i\neq j\\=1}}\tau_i\frac{1}{a}Q_0\tau_j+\cdots|0\rangle. \tag{2.1}$$

τ is a modified-scattering operator defined by

$$\tau_i=v_i+v_ia^{-1}Q_0\tau_i, \tag{2.2}$$

where v_i is the potential between the incident and ith nucleons, $Q_0=1-|0\rangle\langle 0|$ is the nuclear excited-state projector, and

$$a=E_0-H_0+i\epsilon, \tag{2.3}$$

where H_0 is the sum of the incident kinetic-energy operator and the nuclear Hamiltonian; E_0 is the sum of the incident kinetic energy and the nuclear ground-state energy. The operator τ is the scattering operator for the scattering of a particle by a nucleon bound in a nucleus. It is convenient to introduce the operator for the scattering of a particle by a member of a target of independent nucleons,

$$\tau_i'=v_i+v_i(1/a')\tau_i', \tag{2.4}$$

where

$$a'=e_0-h_0+i\epsilon, \tag{2.5}$$

and h_0 is the sum of the kinetic-energy operator of the incident nucleon and those of the nucleons in the target, and e_0 is the corresponding energy eigenvalue. One can easily show that

$$\langle \mathbf{k}';\mathbf{k}_1',\cdots,\mathbf{k}_A'|\tau_i'|\mathbf{k};\mathbf{k}_1,\cdots,\mathbf{k}_A\rangle = \langle \mathbf{k}',\mathbf{k}_i'|t|\mathbf{k},\mathbf{k}_i\rangle\prod_{\substack{j\\j\neq 1}}\delta(\mathbf{k}_j'-\mathbf{k}_j), \tag{2.6}$$

where $\mathbf{k}_i$, $\mathbf{k}_i'$ are initial and final momenta of the struck nucleon, $\mathbf{k}$ and $\mathbf{k}'$ are the initial and final momenta of the incident nucleon, and t is the scattering operator for two free nucleons. Following Kerman, McManus, and Thaler,[10] we eliminate v_i from (2.2) and (2.4) and find

$$\tau_i=\tau_i'+\tau_i'[(1/a)Q_0-1/a']\tau_i, \tag{2.7}$$

which can be iterated to give τ as an expansion in τ'. Keeping only the first term in this expansion, so that $\tau=\tau'$, is called the impulse approximation. Since our aim is to retain all terms in V which are binary or less in t, we examine the second term in the iteration of (2.7);

$$\tau'[a^{-1}Q_0-1/a']\tau'=-\tau'a^{-1}P_0\tau' +\tau'a^{-1}(a'-a)(1/a')\tau', \tag{2.8}$$

where $P_0=|0\rangle\langle 0|$. The difference $(a'-a)$ can be written, using (2.3) and (2.5), as

$$a'-a=u-e_u,$$

where u is the potential energy function of the nucleus and e_u is the shift in the nuclear ground-state energy due to u. However, Brueckner[11] has shown that u can also be expressed in terms of t, so that the second term on the right of (2.8) is of third order in t. Therefore, the second-order correction to the impulse approximation is simply the first term on the right of (2.8). The terms which we will retain in our analysis are therefore

$$\begin{aligned} V^{(1)}&=\langle 0|\sum_i t_i|0\rangle,\\ V_{\mathrm{DS}}{}^{(2)}&=\langle 0|\sum_{i\neq j}t_i\frac{1}{a}Q_0t_j|0\rangle,\\ V_{\mathrm{IA}}{}^{(2)}&=-\langle 0|\sum_i t_i\frac{1}{a}P_0t_i|0\rangle. \end{aligned} \tag{2.9}$$

[10] A. K. Kerman, H. McManus, and R. M. Thaler, Ann. Phys. (N. Y.) 8, 551 (1959).
[11] K. A. Brueckner, Phys. Rev. 100, 36 (1955).

The Schrödinger equation will be numerically solved with a potential given by the sum of the three terms given in (2.9). We expect the effect of the $V^{(2)}$ terms to decrease relative to the $V^{(1)}$ term with increasing incident nucleon energy due to the presence of the $1/a$ term in $V^{(2)}$.

For scattering on the two-nucleon energy shell, the transition matrix t is related to the two-nucleon scattering matrix M by

$$t(q)=-(4\pi\hbar^2/m)M(q), \tag{2.10}$$

where q is the momentum transfer and m is the nucleon mass. The elastic scattering of a nucleon by a nucleus, however, is governed by $A+1$ body kinematics, rather than the two-body kinematics of N-N scattering. Throughout this work, we ignore this difference in energy shells and treat the two-nucleon amplitudes as if they were functions of momentum transfer only. This approximation is exact for forward scattering, and for nonforward scattering at fixed momentum transfer is expected to improve for decreasing target mass number.

Following Stapp,[12] the M matrix may be written as

$$M=[a+c(\boldsymbol{\sigma}_1+\boldsymbol{\sigma}_2)\cdot\hat{n}+b\boldsymbol{\sigma}_1\cdot\hat{n}\boldsymbol{\sigma}_2\cdot\hat{n}+\tfrac{1}{2}(g+h)\boldsymbol{\sigma}_1\cdot\hat{m}\boldsymbol{\sigma}_2\cdot\hat{m} +\tfrac{1}{2}(g-h)\boldsymbol{\sigma}_1\cdot\hat{l}\boldsymbol{\sigma}_2\cdot\hat{l}]+[a'+\cdots]\boldsymbol{\tau}_1\cdot\boldsymbol{\tau}_2, \tag{2.11}$$

where the second bracket is identical in structure to the first, with all functions primed. The quantities $a\cdots e'$ are functions of the momentum transfer q, $\boldsymbol{\sigma}$ and $\boldsymbol{\tau}$ are the spin and isospin operators, respectively, and $\hat{n}$, $\hat{m}$, and $\hat{l}$ are unit vectors in the directions $\mathbf{k}\times\mathbf{k}'$, $\mathbf{k}+\mathbf{k}'$, and $\mathbf{k}-\mathbf{k}'$, where $\mathbf{k}$ and $\mathbf{k}'$ are the initial and final relative wave numbers of the two nucleons.

In momentum space, for $A=2Z$ nuclei, the first term of (2.9), referred to as the "single-scattering" term, is

$$\langle\mathbf{k}'|V^{(1)}|\mathbf{k}\rangle =-(4\pi\hbar^2/m)A[a(q)+c(q)\boldsymbol{\sigma}_0\cdot\hat{n}]F(q), \tag{2.12}$$

where $\mathbf{k}$ and $\mathbf{k}'$ are, respectively, the initial and final relative wave vectors of the nucleon-nucleus system, and $F(q)$ is the nuclear form factor. The approximations made in obtaining (2.12) are the neglect of the momentum distribution of the nuclear nucleons and the use of symmetrized two-nucleon amplitudes rather than the symmetrization of the $A+1$ particle wave function.[13]

We will be concerned with the scattering of nucleons by He^4, C^{12}, and O^{16}. The one-particle densities of these nuclei are well represented by the modified-Gaussian shape of Ehrenberg *et al.*,[14]

$$\rho(r)=\rho_0[1+w(r/a)^2]e^{-(r/a)^2}, \tag{2.13}$$

which yields the form factor

$$F(q)=[1-w(qa)^2/(4+6w)]e^{-(qa)^2/4}.$$

The values of the parameters w and a are taken from Ehrenberg *et al.*[14] and from Fregeau.[15]

In the evaluation of the binary terms of (2.9), we follow Johnston and Watson[8] and neglect the energy differences between the nuclear ground and excited states. This approximation leads to an error[8] of $T/3e(k)$, where $T\cong 30$ MeV is the average kinetic energy of a nuclear nucleon and $e(k)$ is the incident kinetic energy. This approximation enables us to use the closure of the nuclear states in evaluating the binary terms. We also make the assumption of Lax and Feshbach[16] that there are only two pair distribution functions for the nuclear nucleons, corresponding to symmetric and antisymmetric spatial states of two nuclear nucleons. We combine the binary terms of (2.9), calling $V_{\mathrm{DS}}^{(2)}+V_{\mathrm{IA}}^{(2)}=V^{(2)}$, and obtain

$$\langle\mathbf{k}'|V^{(2)}|\mathbf{k}\rangle=\frac{2\mu}{\hbar^2}\frac{1}{(2\pi)^3}\int\frac{d\mathbf{k}}{k^2-K^2+i\epsilon}\int d\mathbf{r}'d\mathbf{r}'' \times e^{-i(\mathbf{q}'\cdot\mathbf{r}'+\mathbf{q}''\cdot\mathbf{r}'')}\rho(\mathbf{r}')\rho(\mathbf{r}'') \times\left[\bar{A}-\bar{C}-\bar{D}+\bar{A}\frac{G^s+G^a}{2}+\bar{B}\frac{G^s-G^a}{2}\right], \tag{2.14}$$

where μ is the reduced nucleon mass, $\mathbf{q}'=\mathbf{k}'-\mathbf{K}$, $\mathbf{q}''=\mathbf{K}-\mathbf{k}$ are the momentum transfers of the successive scatterings, and $G^{s,a}$ are the correlation functions corresponding to symmetric and antisymmetric spatial states of two nuclear nucleons. We assume that the joint distribution function can be written

$$\rho(\mathbf{r}',\mathbf{r}'')=\rho(\mathbf{r}')\rho(\mathbf{r}'')[1+G(|\mathbf{r}'-\mathbf{r}''|)],$$

so that the correlation between two nucleons depends only on their separation and is independent of the location of the pair in the nucleus. The quantities $\bar{A}\cdots\bar{D}$ are averages over the ground-state spin and isospin function $|0)$ of the nucleus:

$$\bar{A}=\sum_{i\neq j}(0|t_it_j|0),$$
$$\bar{B}=\sum_{i\neq j}(0|t_it_jP_{ij}|0),$$
$$\bar{C}=\sum_{i\neq j}(0|t_i|0)(0|t_j|0),$$
$$\bar{D}=\sum_{i}(0|t_i|0)(0|t_i|0).$$

These averages can be written for $A=2Z$ nuclei as[17]

$$\bar{A}=(4\pi\hbar^2/m)^2(A^2\alpha-A\beta),$$
$$\bar{B}=(4\pi\hbar^2/m)^2[4A\alpha-(A^2/4)\beta], \tag{2.15}$$
$$\bar{C}+\bar{D}=(4\pi\hbar^2/m)^2A^2\alpha,$$

[12] H. Stapp, Ann. Rev. Nucl. Sci. **10**, 291 (1960).
[13] G. Takeda and K. M. Watson, Phys. Rev. **97**, 1339 (1955).
[14] H. F. Ehrenberg, R. Hofstadter, U. Meyer-Berkout, D. G. Ravenhall, and S. E. Sobottka, Phys. Rev. **113**, 666 (1959).
[15] H. H. Fregeau, Phys. Rev. **104**, 225 (1956).
[16] M. Lax and H. Feshbach, Phys. Rev. **81**, 189 (1951).
[17] T. K. Fowler and K. M. Watson, Nucl. Phys. **13**, 549 (1959).

where

$$\alpha=a^2+c^2+2ac\boldsymbol{\sigma}_0\cdot\hat{n},$$
$$\beta=[a^2+2c^2+b^2+\tfrac{1}{2}(g^2+h^2)+2c(a+b)\boldsymbol{\sigma}_0\cdot\hat{n}]+3(a'^2+2c'^2+\cdots), \quad (2.16)$$

and where the typical quantity

$$2ac\equiv a(q')c(q'')+a(q'')c(q').$$

The $V_{DS}^{(2)}$ term of Johnston and Watson[8] can be obtained from (2.14) by deletion of $\bar{D}$.

The correlation functions of a nucleus are essentially unknown and must be obtained by assuming a nuclear model. Johnston and Watson[8] find the correlation functions of a Fermi-gas nucleus to be

$$G^s=\frac{\frac{1}{4}A-1}{\frac{1}{4}A+1}G', \qquad G^a=-G', \quad (2.17)$$

where

$$G'=[\tfrac{1}{4}A(\tfrac{1}{4}A-1)]^{-1}\sum_{i\neq j}e^{-i(\mathbf{k}_i-\mathbf{k}_j)\cdot\mathbf{r}},$$

with $\mathbf{r}$ the separation vector of the two nucleons and $\mathbf{k}_i$ an allowed momentum in a Fermi gas. The function G' may readily be evaluated to give

$$G'=(\tfrac{1}{4}AG_F-1)/(\tfrac{1}{4}A-1), \quad (2.18)$$

where

$$G_F(r)=[3j_1(k_Fr)/k_Fr]^2$$

and k_F is the Fermi momentum for a nucleus, 1.27 F^{-1}. The form of (2.18) differs from that of Johnston and Watson, who take $G'\cong G_F$, which is accurate for small r or large A. The correlation function is usually characterized by the correlation length defined by

$$R^{s,a}=\int_0^\infty dr\,G^{s,a}(r).$$

It can be seen from (2.17) and (2.18) that the correlation lengths for a Fermi gas are infinite, which is reasonable since the correlation is due to the Pauli principle, which implies a long-range correlation.

We have also investigated a Brueckner-Gammel (BG)[18] type correlation, which is due primarily to the hard core of the two-nucleon interaction. Fowler and Watson[17] deduced a correlation function from the work of BG and obtained the correlation lengths

$$R^s\cong R^a=-0.84\text{ F}.$$

We have assumed the correlation functions

$$G^s=G^a=G_B, \quad (2.19)$$

where

$$G_B=-e^{-r^2/b^2}(1-\delta r^2/b^2).$$

[18] K. Brueckner and J. Gammel, Phys. Rev. **109**, 1023 (1958).

The normalization condition for large nuclei,

$$\int G_B(r)d\mathbf{r}=0,$$

implies $\delta=\frac{2}{3}$, and requiring

$$\int_0^\infty G_B(r)dr=-0.84\text{ F}$$

implies $b=1.42$ F. It is worth noting that the Fermi-gas correlation is due to the Pauli principle and hence the correlation functions for the symmetric and antisymmetric states are quite different. In the BG model, however, the correlation is mainly due to the hard core of the interaction so that the symmetric and antisymmetric states have essentially the same correlation function.

Using the correlation functions for a Fermi gas as given by Eqs. (2.17) and (2.18) the bracket of (2.14) becomes

$$(4\pi\hbar^2/m)^2(-\tfrac{1}{4}A^2\beta G_F),$$

while for the BG-type correlation functions of Eq. (2.19), the bracket becomes

$$(4\pi\hbar^2/m)^2[-A\beta+(A^2\alpha-A\beta)G_B].$$

The evaluation of (2.14) is complicated by the fact that α and β are functions of the integration variable $\mathbf{K}$. The usual practice[8,9] is to use the forward-scattering values of the two-nucleon amplitudes in calculating α and β. α and β are then taken outside the integral (2.14). This procedure over estimates $V^{(2)}$ because α and β are products of two amplitudes, both of which decrease with increasing momentum transfer. The forward-scattering approximation in fact replaces α and β by their maximum values. To reduce this overestimation of $V^{(2)}$, we set α and β equal to their maximum values subject to the constraint that the initial and final momenta are given by $\mathbf{k}$ and $\mathbf{k}'$. As can be seen from Eq. (2.16), α and β are symmetric in q' and q''. Therefore, if α and β have maximum values, they occur when $q'=q''$. Further, because the two-nucleon amplitudes decrease with increasing momentum transfer, this common value must be as small as possible. It is easily seen that these conditions are met when $\mathbf{K}=\frac{1}{2}(\mathbf{k}+\mathbf{k}')$, so that $\alpha_{\max}=\alpha(\frac{1}{2}q,\frac{1}{2}q)$. $(\alpha,\beta)_{\max}$ are then taken outside the integrals in (2.14) and the integrals completed.

The integrals to be evaluated are of the form

$$I=\frac{1}{(2\pi)^3}\int\frac{d\mathbf{K}}{k^2-K^2+i\epsilon}\int d\mathbf{r}'d\mathbf{r}''e^{-i(\mathbf{q}'\cdot\mathbf{r}'+\mathbf{q}''\cdot\mathbf{r}'')}\times\rho(r')\rho(r'')G(|\mathbf{r}'-\mathbf{r}''|). \quad (2.20)$$

The spatial integrals in (2.18) can be simplified if, instead of the modified Gaussian density of Eq. (2.11),

we take for $\rho(r)$ a simple Gaussian

$$\rho(r)=e^{-r^2/a^2}/\pi^{3/2}a^3, \tag{2.21}$$

with a chosen to give the same rms radius as the corresponding modified Gaussian. (The effect on the observables of using this Gaussian density in $V^{(1)}$ as well is negligible for small momentum transfers. The Gaussian density does, however, produce a less pronounced diffraction minimum than does the corresponding modified Gaussian.)

If we make the change in variables

$$\mathbf{r}=\mathbf{r}'-\mathbf{r}'', \quad \mathbf{R}=\tfrac{1}{2}(\mathbf{r}'+\mathbf{r}'')$$

and note that

$$\frac{1}{(2\pi)^3}\int\frac{d\mathbf{K}\,e^{i\mathbf{K}\cdot\mathbf{r}}}{k^2-K^2+i\epsilon}=-\frac{1}{4\pi}\frac{e^{ikr}}{r},$$

Eq. (2.20) becomes

$$J=-\frac{e^{-(qa)^2/8}}{(2\pi)^{3/2}a^3Q}J, \tag{2.22}$$

where $\mathbf{Q}=\frac{1}{2}(\mathbf{k}'+\mathbf{k})$ and

$$J=\int_0^\infty dr\,e^{-r^2/2a^2+ikr}\sin Qr\,G(r). \tag{2.23}$$

Using the Fermi-correlation functions, we find

$$\langle\mathbf{k}'|V^{(2)}|\mathbf{k}\rangle=\frac{2\mu}{\hbar^2}\frac{e^{-(qa)^2/8}}{(2\pi)^{3/2}a^3Q}\left(\frac{4\pi\hbar^2}{m}\right)^2\frac{A^2}{4}\beta_{\max}J_F \tag{2.24}$$

and the form obtained with the BG correlation functions can be found in a similar way.

In comparing the two-nucleon amplitude with two-nucleon data, partial waves up to some $L_{\max}$ are included. The infinite number of partial waves beyond $L_{\max}$—which are, presumably, accurately represented by the one-pion exchange (OPE) Born approximation—are neglected since they contribute only to the very small momentum-transfer region which is not observable and where, for charged particles, they are completely obscured by the Coulomb interaction. However, Bjorklund *et al.*[19] have suggested that the nucleon-nucleus optical potential could be thought of as the result of repeated small momentum-transfer collisions. We therefore have investigated the effect of including the OPE tail of the two-nucleon amplitudes in the calculation of $V^{(1)}$ following the method of Ref. 19.

The optical potential as obtained in this section is used to solve the partial-wave integral-scattering equation in momentum space. The method of solution and the method of treating Coulomb effects are given in Ref. 4.

[19] F. E. Bjorklund, B. A. Lippmann, and M. J. Moravcsik, Nucl. Phys. **29**, 582 (1962).

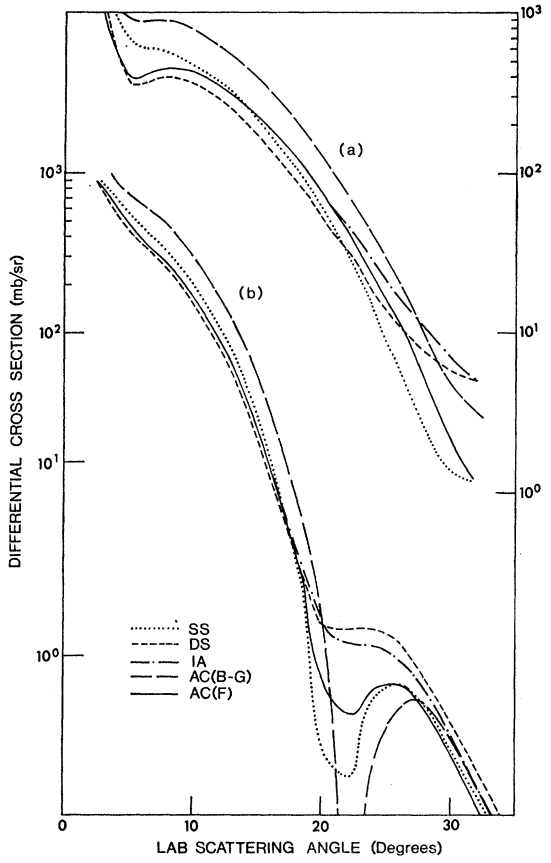

FIG. 1. p-carbon differential cross section at lab energies of (a) 142 MeV, (b) 310 MeV, calculated from the optical potential in the stages SS, DS, IA, AC(B-G), and AC(F), using the Yale phase-shift set.

III. EFFECTS OF THE CORRECTIONS

In this section we examine the effect of the different terms of the optical potential, discussed in Sec. II, on the nucleon-nuclear observables. The complexity of the potential was increased in the following sequence: (i) single scattering (SS); (ii) the addition to SS of the double-scattering correction with the forward-scattering approximation (DS); (iii) the addition to DS of the impulse approximation with the forward-scattering approximation (IA); (iv) elimination of the forward-scattering approximation (EFS); (v) the addition of the OPE tail to EFS (AC). Stages (ii)–(iv) were calculated with the Fermi-correlation function only. The complete potential (v) was calculated for both the Fermi and BG correlation functions.

In Fig. 1, we plot the differential cross section and in Fig. 2 the polarization obtained with the optical potential in the stages SS, DS, IA, AC (Fermi) [AC(F)] and AC (BG). The calculations are made with the Yale[5] phase-shift set for protons incident on carbon at incident energies of 142 and 310 MeV. The qualitative behavior of the curves for the Livermore[6] set is similar. The

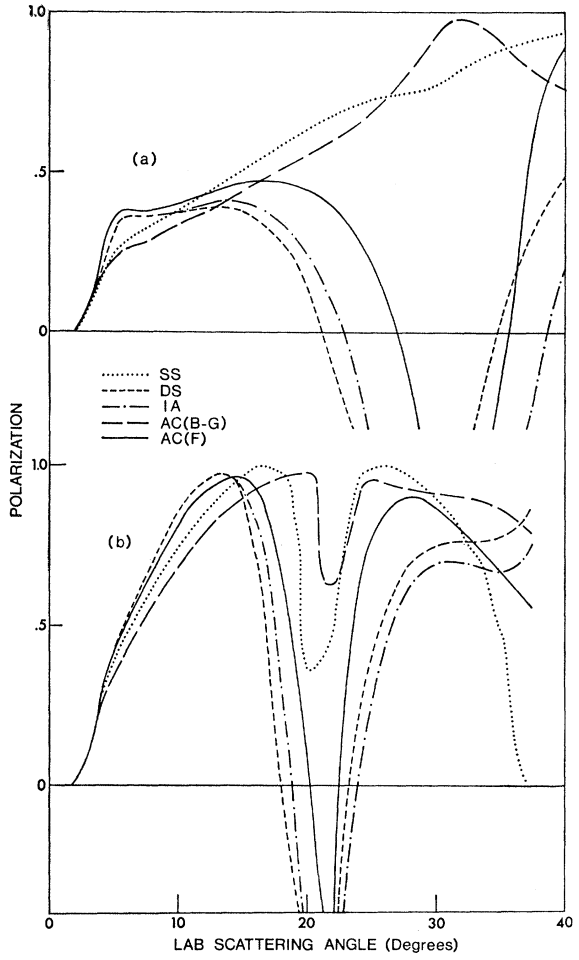

FIG. 2. p-carbon polarization at lab energies of (a) 142 MeV, (b) 310 MeV, calculated from the optical potential in the stages SS, DS, IA, AC(B-G), and AC(F), using the Yale phase-shift set.

curves for EFS cannot be distinguished from those of AC(F) and are not plotted. This indicates that the corrections to the very small momentum-transfer region included in the OPE tail are not necessary in fitting the two-nucleon amplitudes to the nucleon-nuclear data in the region of interest to the present work.

In Fig. 1(a), we see that the DS correction reduces the small-angle scattering and enhances the large-angle scattering when compared to SS, which is what would be expected intuitively. The IA correction raises the small-angle cross section by $\sim 10\%$ and is significant throughout the entire angular range. In comparing IA with AC(F), we see that our method of correcting for the forward-scattering approximation has little effect at small angles but strongly affects the shape of the curves at large angles. As discussed in Sec. II, the forward-scattering approximation over estimates the scattering at finite angles. That is, the AC(F) cross section lies below that for IA and is therefore, closer to the data. We also see that the small-angle cross section for AC(BG) is almost twice that for AC(F) at 142 MeV, which indicates the importance of knowing the correct nuclear-correlation functions.

A notable characteristic of the experimentally observed polarization is the "hole" or large dip which occurs in the vicinity of the cross-section diffraction minimum. This hole is an aspect of multiple scattering and an indication of nuclear structure; it does not appear in Born-approximation polarization calculations which are independent of nuclear structure or form factors.[3] In Fig. 2(a) we note that the SS potential does not give rise to the polarization hole at 142 MeV. The hole appears only when the binary corrections are added, and then only with the Fermi correlation functions and not with the BG functions. This phenomenon may be understood qualitatively by noting that the SS polarization is near maximum at the cross-section diffraction

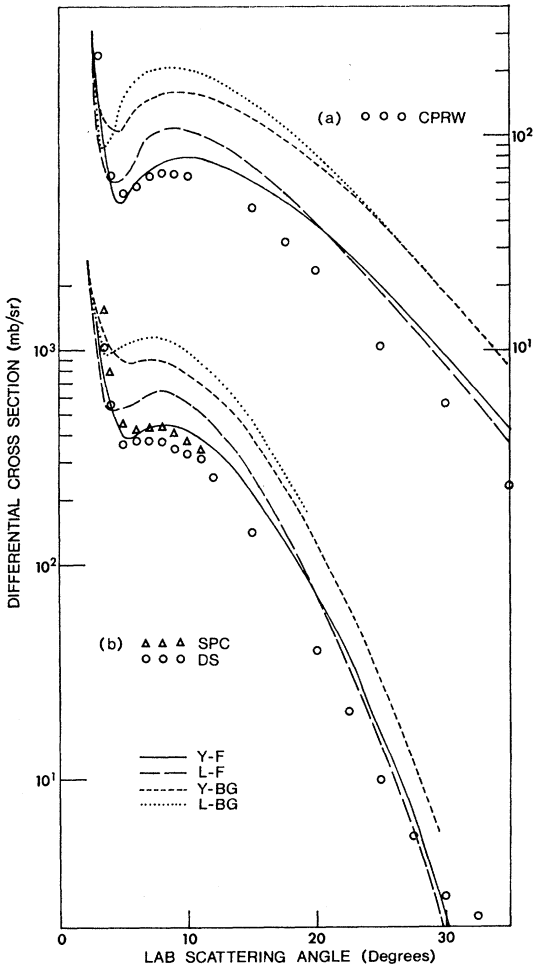

FIG. 3. Calculated differential cross section versus data at an incident lab energy of 142 MeV. (a) p-He elastic scattering, data marked by circles from CPRW. (b) p-C elastic scattering, data marked by triangles from SPC, and by circles from DS. In this and succeeding figures, error bars are not drawn where quoted statistical errors are smaller than data symbol.

minimum. There is a large difference between the scattering of nucleons whose spin is perpendicular to the scattering plane in a left-handed manner and those whose spin is right-handed. The double-scattering contribution is opposite in sign to the single-scattering amplitude; if the correlation is spin-independent, it will subtract roughly equally from the left-handed and right-handed spin amplitudes, thus leaving the difference and hence the polarization unchanged. This latter situation is characteristic of the BG correlation functions which are the same for spatially symmetric and spatially antisymmetric nuclear pairs in the nucleus, i.e., for singlet and triplet target pairs. The Fermi-correlation functions, being opposite in sign for singlet and triplet target states, can lead to a diminution of the spin-amplitude difference and hence to a dip in the polarization. This situation would be most marked at the diffraction minimum, where the single-scattering amplitudes become small enough to be comparable with the double-scattering amplitudes, as is observed.

Also apparent is the pronounced effect on the polarization at large angles due to the removal of the forward-scattering approximation; this is correlated with the expected reduction in the large-angle cross section as seen in Fig. 1(a).

A comparison of Figs. 1(a) and 1(b) indicates that all of the corrections decrease with increasing energy of the incident particle, as expected. At 310 MeV, the cross section is well represented by the SS curve. The same trend can also be seen in the polarization curves, Figs. 2(a) and 2(b).

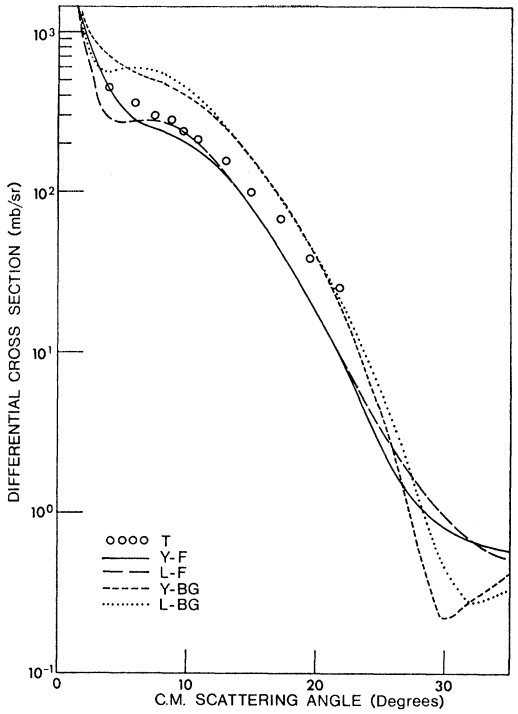

FIG. 5. Calculated differential cross section versus data for p-C elastic scattering at an incident lab energy of 210 MeV. Data marked by circles are from T.

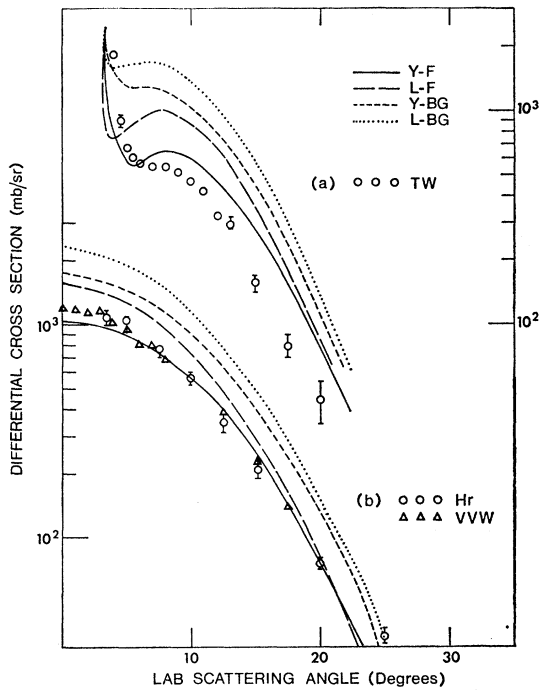

FIG. 4. Calculated differential cross section versus data at an incident lab energy of 142 MeV. (a) p-O elastic-scattering data, marked by circles from TW. (b) n-C elastic scattering, data marked by circles from Hr, and by triangles from VVW.

At the SS and DS stages we were able to compare our work with that of McDonald and Hull,[9] who calculated the small-angle cross section and polarization for p-C scattering at 142 and 310 MeV using the Yale set. We found[4] that our SS cross sections and polarizations at both energies are essentially identical to theirs. At 142 MeV, our DS cross section is again identical to theirs; however, our DS polarization lies above, and closer to the data, than does our SS polarization, whereas McDonald and Hull find the SS and DS polarizations to be the same at small angles for this energy. At 310 MeV, our DS cross section lies below our SS, while in Ref. 9 the DS cross section lies slightly above the SS. The 310-MeV polarizations are difficult to compare because of the closeness of the curves. Of the several details in which our calculation differs from that of McDonald and Hull, it is difficult to single out one as giving rise to the differences in calculated observables just noted. However, it should be noted that McDonald and Hull make the approximation of using a correlation length, whereas we stick to the more fundamental correlation function. Furthermore, we use the exact relation (2.18), whereas they assume $G'=G_J$ which is likely to be a quite erroneous representation of (2.18) for the values of A of interest here.

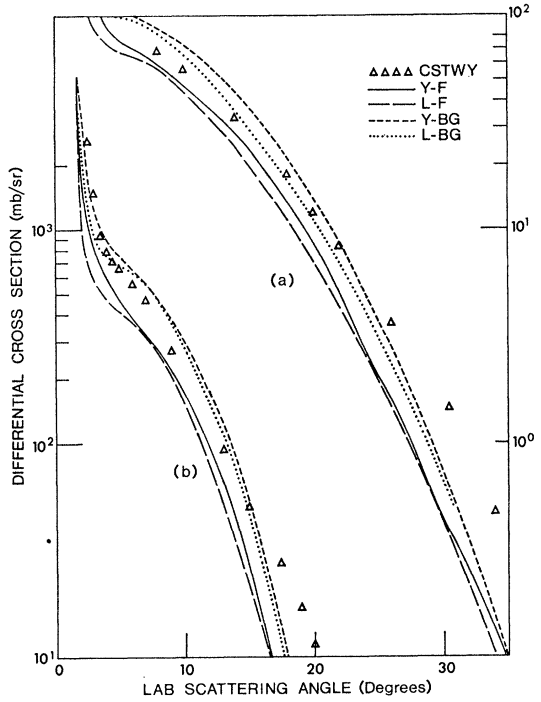

FIG. 6. Calculated differential cross section versus data at an incident lab energy of 310 MeV. (a) p-He elastic scattering. (b) p-C elastic scattering. Data marked by triangles in (a) and (b) are from CSTWY.

IV. COMPARISON WITH DATA

In this section, we compare our calculations with nucleon-nuclear elastic-scattering data. Our primary purpose here is to attempt to choose between the Yale[5] (Y) and Livermore[6] (L) phase-parameter sets on the basis of this comparison. Before this can be done, however, we must decide whether the Fermi (F) or BG correlation functions more closely resemble the actual correlation functions. The calculations used for comparison with data in this section include all of the corrections discussed in Sec. II; they are designated AC in Sec. III.

Differential Cross Section

142 MeV. Figure 3(a) shows the p-He differential cross section. The data are from Cormack *et al.*[20] (CPRW). The Y-F curve gives a reasonable fit to the data to $\sim 10°$, while the L-F curve is almost a factor of two too high in this range. The Y-BG and L-BG curves lie even higher.

Figure 3(b) shows the p-C differential cross section. The data are those Steinberg *et al.*[21] (SPC), and of Dickson and Salter[22] (DS). The SPC data are corrected for multiple Coulomb scattering in the target and are believed to have a systematic error of 3% or less; they are, by far, the best data we have found. As can be seen, the Y-F curve fits the data quite well, especially the SPC data. The L-F curve is $\sim 50\%$ high in the small-angle region and Y-BG and L-BG are $\sim 100\%$ high in this region.

Figure 4(a) shows the p-O differential cross section. The data are those of Taylor and Wood[23] (TW). Again, it is the Y-F curve which best fits the data; with the L-F curve high by a factor of almost 2.

Figure 4(b) shows the n-C differential cross section, with data from Harding[24] (Hr) and Voss, VanZyl, and Wilson[25] (VVW). Here, also, the Y-F fits the data very well to $\sim 20°$, while the L-F curve is $\sim 25\%$ high at 0°.

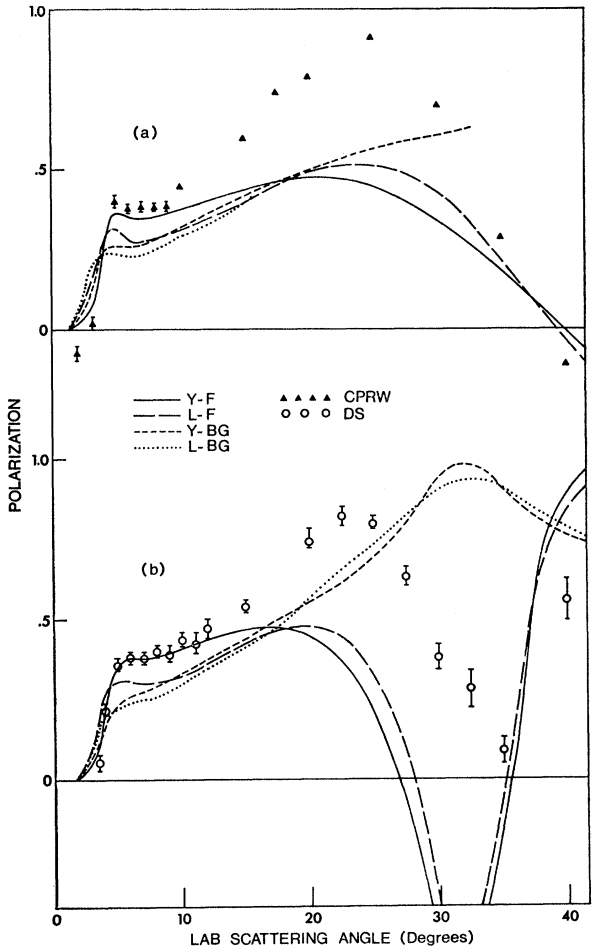

FIG. 7. Calculated polarization versus data at an incident energy of 142 MeV. (a) p-He elastic scattering, data marked by triangles from CPRW. (b) p-C elastic scattering, data marked by circles from DS.

[20] A. M. Cormack, J. N. Palmieri, N. F. Ramsey, and R. Wilson, Phys. Rev. **115**, 599 (1955).
[21] D. Steinberg, J. N. Palmieri, and A. M. Cormack, Nucl. Phys. **56**, 46 (1964).
[22] J. M. Dickson and D. C. Salter, Nuovo Cimento **6**, 235 (1957).
[23] A. E. Taylor and E. Wood, Nucl. Phys. **25**, 642 (1961).
[24] R. S. Harding, Phys. Rev. **111**, 1164 (1958).
[25] C. P. VanZyl, R. G. P. Voss, and R. Wilson, Phil. Mag. **1**, 1003 (1956).

210 MeV. Figure 5 shows the p-C differential cross section with the data from Thwaites[26] (T). We can see that the L-F and L-BG curves show excessive destructive Coulomb interference. The Y-F curve is about 20% low in this region, while the Y-BG curve is about 50% high.

310 MeV. Figures 6(a) shows the p-He cross-section fits, with the data of Chamberlain *et al.*[27] (CSTWY). All of the curves fit the small-angle data fairly well, although the L-F and Y-F curves lie somewhat closer to the data than the corresponding BG curves.

Figure 6(b) shows the p-C cross-section fits, with the data of CSTWY. This is the only case we have found in which the BG fits are closer to the data than the F fits. We can see that the L-F and L-BG fits both show more Coulomb interference than do the data. It should be mentioned that Batty[28] has questioned the normalization of the small-angle CSTWY data which include the data to 7°.

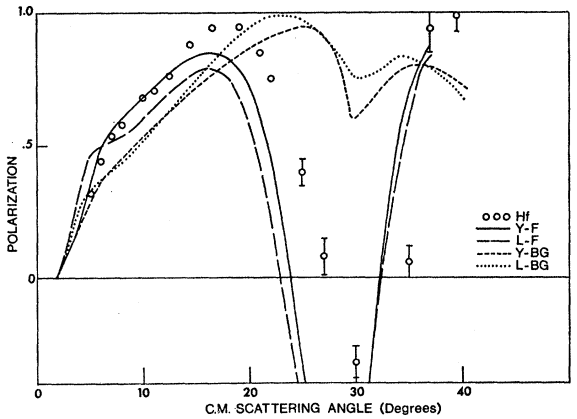

FIG. 9. Calculated polarization versus data for p-C elastic scattering at an incident lab energy at 210 MeV. Data marked by circles from Hf.

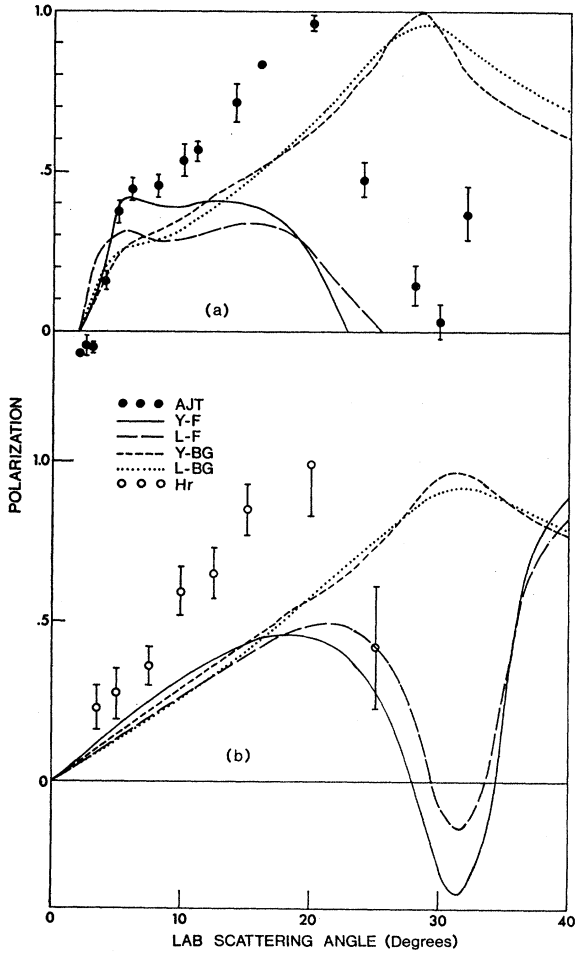

FIG. 8. Calculated polarization versus data at 142 MeV. (a) p-O elastic scattering, data marked by circles from AJT. (b) n-C elastic scattering, data marked by circles from Hr.

Polarization

142 MeV. Figures 7(a), (7b), 8(a) show the polarization for p-He, p-C, p-O, and n-C scattering. The p-O data are from Alphonce *et al.*[29] (AJT). All of the 142-MeV data lead to the same conclusion: The small-angle polarization is best fit by the Y-F curves. It is also striking that neither of the BG curves shows the characteristic hole in the polarization at the diffraction minimum, which is exhibited by both of the F curves and by the data. (In Fig. 7, the data have been adjusted downward, following Jarvis and Rose.[30])

210 MeV. Figure 9 shows the p-C polarization at 210 MeV; the data are from Hafner[31] (Hf). The Y-F fit is extremely good to ~14°. The L-F and L-BG fits show excessive Coulomb interference. Again, the BG curves do not have the deep hole at the diffraction minimum, which seems to be required by the data and which is shown by the F curves.

310 MeV. Figures 10(a) and 10(b) show the p-He and p-C polarization at 310 MeV. It is difficult to make a comparison of the fits because the small-angle fits all lie very close together. We see that the F curves come down faster at the diffraction minimum than do the BG curves and are thus more similar to the data variation at larger angles.

Correlation Functions

The fits at 142 and 210 MeV strongly favor the Fermi-correlation functions and the polarization at 310 MeV

[26] T. T. Thwaites, Ann. Phys. (N. Y.) **12**, 56 (1961).
[27] O. Chamberlain, E. Segrè, R. D. Tripp, C. Wiegand, and T. Ypsilantis, Phys. Rev. **102**, 1659 (1956).
[28] C. J. Batty, Nucl. Phys. **23**, 562 (1962).
[29] R. Alphonce, A. Johansson, and G. Tibell, Nucl. Phys. **4**, 672 (1957).
[30] O. N. Jarvis and B. Rose, Phys. Letters **15**, 271 (1965).
[31] E. M. Hafner, Phys. Rev. **111**, 297 (1958).

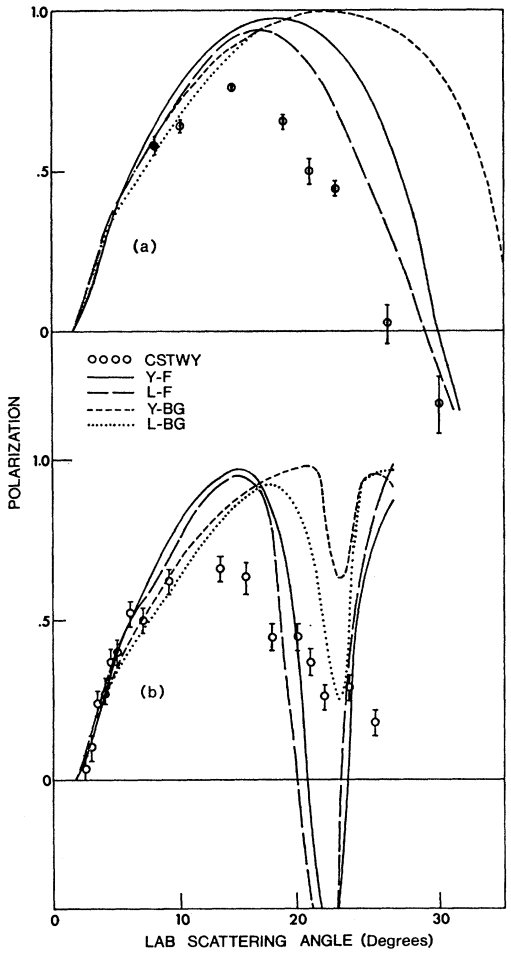

FIG. 10. Calculated polarization versus data at an incident lab energy of 310 MeV. (a) p-He elastic scattering. (b) p-C elastic scattering. Data marked by circles in (a) and (b) are from CSTWY.

is certainly consistent with such a choice. From the form of the function J [Eq. (2.21)] in which the correlation functions G appear, we can that it is the value of $G(r)$ at intermediate separations which most strongly affects the optical potential; the integrand of J is damped by an exponential at large r and by a sine at small r. Therefore we conclude that the Fermi-correlation functions more closely resemble the true correlation functions in the intermediate range of r than do the BG functions, i.e., there *is* a significant difference between the spatially even and odd two-nucleon correlation functions. McDonald and Hull[9] believe that their calculation favors the BG functions, but their calculation is not extended to angles large enough to make the polarization hole apparent. Furthermore, as discussed in Sec. II, our calculation differs from theirs in the inclusion of the impulse-approximation correction as well as the modification of the forward-scattering approximation and the use of the correlation functions rather than simply the correlation lengths.

In our comparison of the Yale and Livermore phase parameters, we will proceed on the premise that the Fermi-correlation functions are the best available.

Comparison of Phase-Parameter Sets

At 142 MeV, we found that the Yale set gave a decidedly better fit to the p-He, p-C, p-O, and n-C data, both differential cross section and polarization, than did the Livermore set. We therefore conclude that our calculation favors the Yale over the Livermore set at this energy.

At 210 MeV, the Yale set gave a very good fit to the p-C polarization and gave the qualitative behavior of the differential cross section as well. The Livermore set, on the other hand, gave rise to excessive Coulomb interference in both observables. We conclude that our calculation favors the Yale set over the Livermore set at 210 MeV.

At 310 MeV, the Yale set gives a slightly better p-He cross section than does the Livermore set. For the p-C cross section, the Yale fit is good to $\sim 5°$, where it falls below the data. The Livermore p-C fit shows more Coulomb interference than do the data and lies below the Yale fit to about 6°. As can be seen from Fig. 10, the polarization fits are inconclusive. We therefore conclude that our calculation favors the Yale set over the Livermore set at 310 MeV as well, although not as strongly as at the lower energies.

V. FACTORS WHICH AFFECT AGREEMENT WITH DATA

In this section we explore the question of why our agreement with data does not extend over a larger angular range. In comparing Figs. 1(a) and 1(b) and 2(a) and 2(b) we see that the effect of $V^{(2)}$ relative to that of $V^{(1)}$ decreases with increasing energy. It seems reasonable to ascribe most of the decrease in accuracy of the large-angle fits at 310 MeV to the approximations made in obtaining $V^{(1)}$. These are (i) lack of symmetrization of the $A+1$ particle wave function, (ii) neglect of target nucleon momentum, and (iii) energy-shell approximation. The first two approximations have been estimated[9] to give errors of $\sim 3\%$ each at 100 MeV, and cannot account for the large-angle discrepancies at 310 MeV.

The energy-shell approximation is exact for forward scattering and, for nonforward scattering, is expected to improve at a fixed angle of scattering with decreasing mass number of the target. If we compare the p-He and p-C differential cross sections in Figs. 6(c) and 6(b), we can see that the calculated p-He cross section begins to get poor at $\sim 20°$ in the lab frame, corresponding to a momentum transfer of ~ 1.4 F^{-1}, while the p-C cross section gets poor at $\sim 5°$ in the lab, for a momentum transfer of ~ 0.4 F^{-1}.

A similar comparison at 142 MeV cannot be made because the binary potential is significant with respect

to the single-scattering potential. In addition to the approximations made for the first-order potential, additional approximations have been made in the evaluation of the second-order potential, which makes it difficult to isolate the cause of the poor large-angle fits at 142 MeV.

The results at 310 MeV, however, strongly indicate that the off-energy shell behavior of the two-nucleon amplitudes must be taken into account if a better fit to the data over a larger angular region is to be obtained.

VI. CONCLUSION

In this work, we have calculated the optical potential to second order in the two-nucleon scattering amplitudes. This required the evaluation of double scattering and impulse-approximation corrections. Corrections to the impulse approximation had not been included in previous efforts in this area.[9] In addition, we have partially removed the forward-scattering approximation in evaluating the binary potential. We have also evaluated the integrals over the correlation functions rather than approximating them by correlation lengths, as is usually done.

By comparing the resultant calculated observables with experiment for several nuclei at incident energies of 142, 210, and 310 MeV, we concluded that, except for the proton-carbon cross section at 310 MeV, the Fermi-correlation functions were definitely superior to the BG correlation functions insofar as they appear in the calculation of the binary potential. Since this superiority holds for both sets of phase shifts, we infer that some information is obtainable from elastic scattering data about nucleon correlations without conclusive *a priori* information about the N-N interaction, Taking the Fermi- correlation functions as the better representation of the actual correlation at intermediate N-N distances in the nucleus, we find that a reasonably clear distinction is possible between different N-N phase-shift sets and that the Yale set gives a better fit to the data than the Livermore set at all three of the energies investigated.

In order to obtain high-quality fits to the data at the larger angles, it appears that a major program for understanding off-energy shell effects will have to be undertaken. However, there does seem to be an intermediate range of scattering angles where energy-shell uncertainties are not yet sufficiently important and where it is possible to draw distinctions between the different available sets of N-N scattering phase shifts. It is hoped that further improvements in the search procedures for the N-N parameters (such as the newer Yale fits 5) will lead to sets which allow precision fitting of the nucleon-nucleus data in the intermediate angle range just mentioned. Such precision fits would be the obvious starting point for investigations of off-energy-shell effects, which should then lead to improvement in the fits over the entire angular range considered in this paper.

ACKNOWLEDGMENTS

We would like to express our appreciation to the Computing and Data Processing Center, Wayne State University, for making computing time available for this work. Also, one of the authors (A.M.S.) wishes to acknowledge the hospitality of the Aspen Institute for Humanistic Studies, Physics Division.